The Journal of Chemical Physics ARTICLE pubs.aip.org/aip/jcp

Dynamics of viscous liquids and the random barrier model

Cite as: J. Chem. Phys. 165, 064512 (2026); doi: 10.1063/5.0336682
Submitted: 1 April 2026 • Accepted: 26 June 2026 •
Published Online: 12 August 2026

Thomas B. Schrøder,[1,a] Jeppe C. Dyre,[1,b] and Camille Scalliet[2,c]

AFFILIATIONS

[1] "Glass and Time," IMFUFA, Department of Science and Environment, Roskilde University, P.O. Box 260, DK-4000 Roskilde, Denmark
[2] Laboratoire de Physique de l'Ecole Normale Supérieure, ENS, Université PSL, CNRS, Sorbonne Université, Université de Paris, F-75005 Paris, France

[a] **Author to whom correspondence should be addressed:** tbs@ruc.dk
[b] dyre@ruc.dk
[c] camille.scalliet@ens.fr

ABSTRACT

This paper combines the particle-swap Monte Carlo algorithm with long GPU molecular dynamics simulations to analyze the dynamics of a ternary Lennard-Jones glass-forming liquid in the extremely viscous regime. The focus is on the inherent dynamics, obtained by quenching configurations along the configuration-space trajectory into their inherent state. We compare how two functional forms, the von Schweidler law and the prediction of the random barrier model (RBM) in the extreme disorder limit, fit data for the inherent mean-square displacement as a function of time. We find that the RBM, which has no dimensionless free parameters, generally fits the data better than the von Schweidler law, despite the latter's one dimensionless free parameter. In particular, this implies that the RBM predicts the value of the diffusion coefficient from short-time simulation data more accurately than does the von Schweidler expression. Furthermore, we find that the RBM also fits very well the inherent mean-square displacement of a polydisperse Lennard-Jones mixture. It remains an open question why the RBM reproduces well the data despite this model's (unrealistic) assumption of identical energy minima.

I. INTRODUCTION

Experimental works of Gainaru and co-workers highlighted a possible universality of the complex frequency-dependent fluidity of non-polymeric viscous liquids (the inverse of the shear viscosity).[1,2] For nine quite different glass-formers—including van der Waals, ionic, and hydrogen-bonding liquids—the real part of the fluidity was found to be very similar as a function of frequency. This universal shape was found to be well described by the extreme disorder limit of the random barrier model (RBM). Subsequent simulations showed that the RBM fits also the mean-square displacement (MSD) of a simple binary glass-forming liquid.[3] In particular, the so-called *inherent* MSD,[4] where the MSD short-time plateau deriving from thermal vibrations is not present, was found also to be well fitted by the RBM prediction, which has no free shape parameters.

The RBM was proposed as an idealized model of ac conduction in amorphous solids.[5,6] The model considers independent particles jumping between nearest-neighbor same-energy sites of a cubic lattice with energy barriers drawn from some probability distribution. By reference to percolation, the model was later solved in the extreme disorder limit of the effective-medium approximation (EMA), i.e., at low temperatures where the jump rates cover many decades, and the analytical solution agrees very well with numerical results.[7]

The experimental and simulation results described above suggest universality in the motion of atoms or molecules in highly viscous liquids. This raises two questions: (i) The picture of quenched disorder with identical site energies, as in the RBM, is not how one usually thinks about liquids, neither in 3d space, nor in the high-dimensional configuration space. To the contrary, viscous liquids are well known to have a broad distribution of inherent state energies (potential-energy minima) leading to a higher specific heat in the liquid than in the glass phase. So, why does the RBM describe viscous liquid dynamics well? (ii) The dynamics of viscous

liquids has been studied for many years, both in experiments and in simulations; why has the apparent RBM universality not been observed before?

In this article, we present simulations of a ternary glass former carried out in order to illuminate these questions. Thanks to the addition of a third particle type compared to the model investigated in Ref. 3, the liquid can be equilibrated efficiently down to lower temperatures. We test the agreement with the RBM by performing simulations down to temperatures at which the dynamics is roughly 30 times slower than those investigated in Ref. 3. This is done by combining state-of-the-art numerical techniques. Specifically, we take advantage of a recent extension of the swap algorithm to a model of metallic glasses in order to generate equilibrium configurations at very low temperatures,[8] which is combined with state-of-the-art graphics-processing unit (GPU) molecular-dynamics simulations that efficiently access equilibrium dynamics at low temperatures over long time scales.[9]

II. METHODS

A. Model

We study a three-dimensional model for metallic glasses, employing the ternary mixture developed in Ref. 8. This model extends the well-known Kob–Andersen (KA) model[10] by adding a third particle type, which ensures resistance against crystallization and increased efficiency for equilibration with particle-swap dynamics, as detailed in Ref. 8 where the model is referred to as KA_2.

The KA_2 model involves three particle types, A (large), B (small), and C (medium), in the ratio A:B:C = 4:1:1. Two particles i and j at positions $\mathbf{r}_i$ and $\mathbf{r}_j$, separated by the distance $r = |\mathbf{r}_i - \mathbf{r}_j|$, interact via a smoothed Lennard-Jones (LJ) potential,

$$v_{ij}(r) = 4\epsilon_{ij}\left[\left(\frac{\sigma_{ij}}{r}\right)^{12} - \left(\frac{\sigma_{ij}}{r}\right)^{6}\right] + S_{ij}(r), \tag{1}$$

whenever $r < 2.5\sigma_{ij}$. The smoothing polynomial removing discontinuities resulting from the truncation is given by

$$S_{ij}(r) = 4\epsilon_{ij}\left[C_0 + C_2\left(\frac{r}{\sigma_{ij}}\right)^{2} + C_4\left(\frac{r}{\sigma_{ij}}\right)^{4}\right]. \tag{2}$$

Here, $C_0 = 10/r_c^6 - 28/r_c^{12}$, $C_2 = 48/r_c^{14} - 15/r_c^8$, and $C_4 = 6/r_c^{10} - 21/r_c^{16}$ ensure continuity of the potential $v_{ij}(r)$ and its first two derivatives at the cutoff distance $r_c \equiv 2.5\sigma_{ij}$.

The unit length is σ_{AA} and the unit energy is ϵ_{AA}, henceforth just denoted σ and ϵ. In terms of these quantities, the remaining interaction parameters are $\epsilon_{AB} = 1.5\epsilon$, $\epsilon_{AC} = 1.25\epsilon$, $\epsilon_{BB} = 0.5\epsilon$, $\epsilon_{BC} = 1.00\epsilon$, and $\epsilon_{CC} = 0.75\epsilon$ for the energies; and $\sigma_{AB} = 0.8\sigma$, $\sigma_{AC} = 0.9\sigma$, $\sigma_{BB} = 0.88\sigma$, $\sigma_{BC} = 0.84\sigma$ and $\sigma_{CC} = 0.94\sigma$ for the interaction ranges. All particles have the same mass m. The time unit is $\tau_{LJ} = \sqrt{m\sigma^2/\epsilon}$.

We simulated $N = 12\,000$ particles at number density $\rho = N/L^3 = 1.35$ in a cubic box of linear size L with periodic boundary conditions. This particle density is higher than the commonly investigated $\rho = 1.2$,[10] which is motivated by the fact that the average particle size of the KA_2 model is slightly smaller than that of the standard KA model. Indeed, for $\rho = 1.2$, the attractive potential gives rise to a liquid–gas spinodal at low temperature that may intersect the glass transition line,[11] leading to a gas–glass instability.[12] Choosing $\rho = 1.35$ ensures stability of the liquid, as well as positive pressure at equilibrium at the corresponding inherent states down to the lowest temperatures investigated ($T = 0.509$).

The temperature scales relevant for this model at $\rho = 1.35$ were discussed in Ref. 13. They are obtained from the structural relaxation time τ_α extracted from the self-intermediate scattering function by $F_s(q, t = \tau_\alpha) = 1/e$. The function is averaged over a shell of wave vectors with modulus $q = 7.2 \pm 0.05$. The onset of glassy dynamics occurs around $T_o \simeq 1.0$, signaled by τ_α departing from the high-temperature Arrhenius behavior. The putative mode-coupling transition temperature, T_{mct}, is obtained by fitting the relaxation times at moderate supercooling with a power law, $\tau_\alpha \propto (T - T_{\mathrm{mct}})^{-\gamma}$, resulting in $T_{\mathrm{mct}} \cong 0.62$ (with the best fit parameter $\gamma = 2.7$). The lowest temperature studied is $T = 0.509$ at which the alpha-relaxation time is estimated to be four orders of magnitude larger than at T_{mct}.

B. Simulation methods

We first generated equilibrium configurations of the model at various temperatures. This was done using the hybrid molecular dynamics/particle-swap Monte Carlo algorithm implemented in the LAMMPS package.[14] Based on Ref. 8, we have found that short blocks of 10 MD steps with a time step $dt = 5 \times 10^{-3}$ interspersed with blocks of $1.75N = 21\,000$ attempted particle swap moves yields the most efficient dynamical speedup. At each temperature, we performed long equilibration runs ensuring the absence of aging in the dynamics and proper convergence of potential energy and relaxation time. We generated 20 independent equilibrium configurations at each temperature.

Next, we investigated the equilibrium relaxation dynamics via standard molecular dynamics, i.e., without particle swaps. This was done utilizing state-of-the-art graphics-processing unit (GPU)

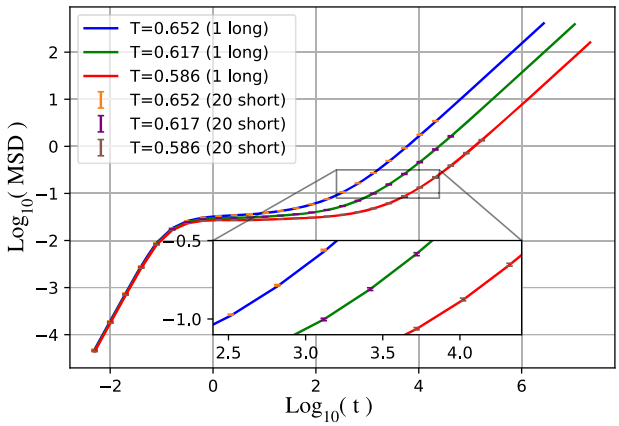

FIG. 1. All-particle mean-square displacement (MSD) as a function of time in a log–log plot at the three highest temperatures studied. Full lines: Results of MD simulations preceded by a MD equilibration run of same length. Data points: Results averaged over 20 independent short MD simulations, each initiated by an equilibrium configuration generated by particle-swap. The error bars indicate one-standard-deviation error estimates. As expected, the dynamics is the same within the error bars.

simulations to access equilibrium dynamics at very low temperatures over unprecedented long times.[9] These Newtonian molecular dynamics (MD) simulations were run in the *NVT* ensemble using a Nose–Hoover thermostat to control the temperature. The equations of motion were integrated with the time step $dt = 0.005$. The algorithm allows one to reach a simulation time of 4.3×10^7 (8.6×10^9 time steps) in 210 h for each of the 20 independent samples of $N = 12\,000$ particles.

C. Observables

The central observable in this work is the mean-square displacement as a function of time, $\langle \Delta r^2(t) \rangle$. This quantity is defined as

$$\langle \Delta r^2(t) \rangle = \frac{1}{N} \left\langle \sum_{i=1}^{N} |\mathbf{r}_i(t) - \mathbf{r}_i(0)|^2 \right\rangle, \tag{3}$$

in which the sharp brackets indicate an average over independent simulations and different initial times. The independent simulations were obtained either from a single very long MD trajectory (at higher temperatures) or from independent initial equilibrium configurations (at low temperatures). We present in this paper data for the MSD both averaged over all particles and restricted to a single particle type (A, B, or C).

At short times and low temperatures, the MSD is dominated by vibrations of the particles inside the cage formed by their neighbors. This hides a weak signal emerging from a few cage-breaking relaxation events. In order to filter out these intra-cage vibrations, we follow the procedure of Refs. 3 and 4 and compute the inherent state (IS) MSD, $\langle \Delta r_I^2(t) \rangle$. Recall that the inherent state is arrived at by quenching to the nearest potential-energy minimum[15] and that "inherent dynamics" is defined as the sequence of inherent states traced out by quenching all states of the "true" dynamics.[4] The inherent dynamics then defines the IS MSD, which is a continuous function of time despite the fact that the inherent dynamics itself is discontinuous. The IS MSD is computed simply by replacing the particle positions $\mathbf{r}_i(t)$ in Eq. (3) by their inherent-state positions, $\mathbf{r}_{i,I}(t)$, identified by the standard conjugate-gradient method. The IS MSD computation can, of course, like the MSD itself, be evaluated by averaging over all particles or restricted to a given particle type.

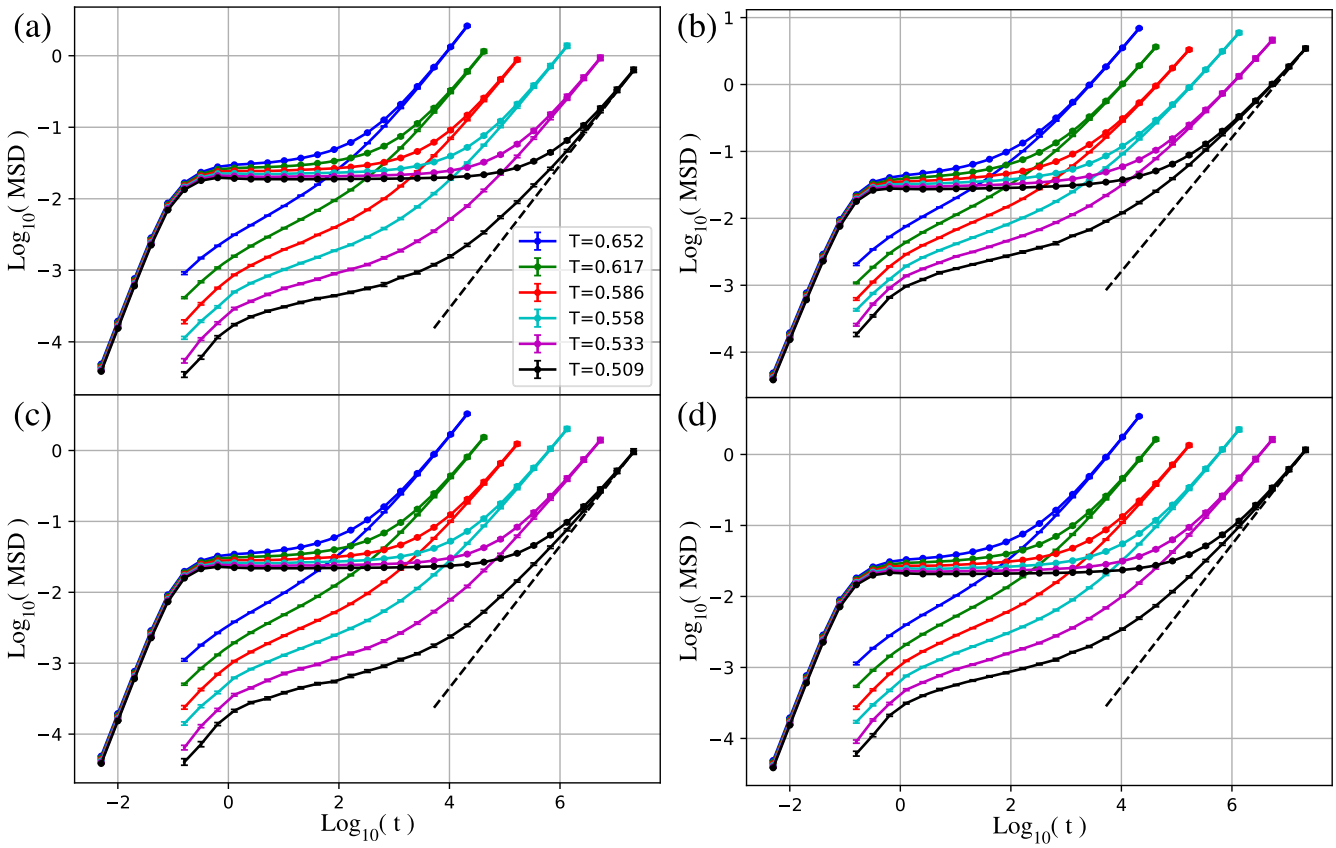

FIG. 2. Mean-square displacement as a function of time in log-log plots for (a) A, (b) B, (c) C, and (d) all particles at the temperatures studied. All initial configurations were equilibrated by swap. For each temperature, two curves are shown: The thermal MSD (for the all-particle three highest temperature these are the same data as in Fig. 1), and the corresponding inherent dynamics.

III. RESULTS

We investigate as mentioned the slow dynamics of the liquid by evaluating the mean-square displacement (MSD) of particles as a function of time, $\langle \Delta r^2(t) \rangle$.

A. Validation of the numerical strategy

Figure 1 shows the all-particle MSD at the three highest temperatures. These data were obtained by two routes. The full lines mark the MSD measured over a single long MD simulation, which was preceded by an equally long equilibration simulation. The points represent the data obtained by starting 20 MD simulations from independent configurations generated via the particle-swap algorithm. At all temperatures, the two curves overlap within the error bars (inset). This confirms that equilibration by particle swap and long MD simulations yield the same results. At temperatures lower than $T \cong 0.59$, brute-force long MD simulations can no longer reach equilibrium and particle-swap methods are necessary because of the extremely long MD equilibration times.

B. Thermal and inherent MSD results

Figure 2 shows the MSD at six temperatures, four of which are significantly below $T_{\mathrm{mct}} \cong 0.62$. The figure shows data averaged over each particle type (A, B, or C) separately, as well as over all particles [panel (d)]. All temperatures investigated in this figure are in the viscous regime. The MSD curves exhibit the same qualitative behavior: The dynamics is ballistic at very short times before the particles collide with nearest neighbors, resulting in a transient caging. From the microscopic time scale $t \simeq 1$ and onward (in simulation units), the MSD reaches a plateau reflecting that the main motion is of a vibrational nature. The plateau length increases with decreasing temperature and reaches five decades at the lowest temperature investigated. At long times, the MSD data cross over to diffusive behavior, $\langle \Delta r^2(t) \rangle \propto 6Dt$ (dashed lines), in which D is the (temperature-dependent) diffusion coefficient.

As previously mentioned,[3,16] the IS MSD is non-zero and increases with time also in the MSD plateau regime. The interpretation is that the IS MSD removes the effect of thermal vibrations leading to the plateau.[3,4] This obviously only applies at time scales where the plateau is well established, and consequently we will in the following only analyze the IS MSD for times $t > 10$. The IS MSD being non-zero and increasing with time in the plateau regime reflects that structural rearrangements occur already at short times and that these accumulate over time. At long times, all particles have undergone structural rearrangements and the thermal and inherent MSDs coincide.

C. Fitting the inherent MSD

Next, we focus on the IS MSD in order to investigate the validity and predictability of two fitting forms, the von Schweidler law and the Random Barrier Model.

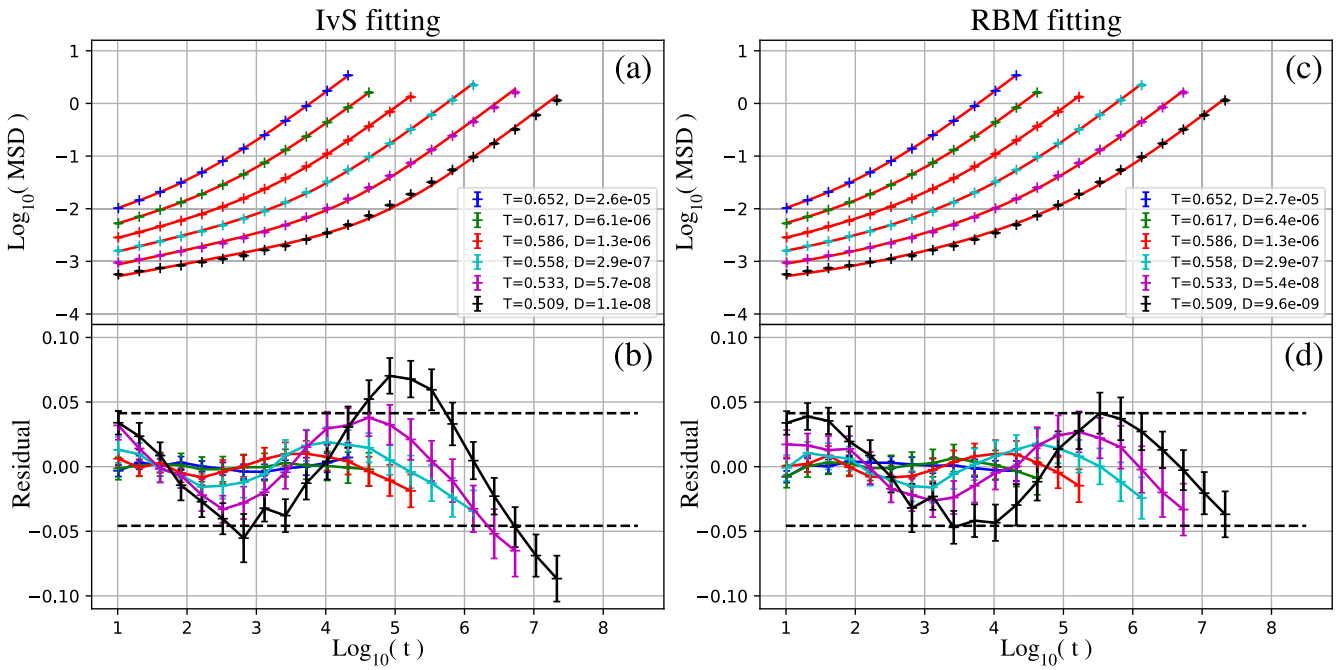

FIG. 3. Fits [(a) and (c)] and residuals [(b) and (d)] for the inherent all-particle MSD data (crosses). [(a) and (b)] Fitting to the inherent von Schweidler law [IvS, Eq. (5)]. [(c) and (d)] Fitting to the Random Barrier Model [RBM, Eq. (A1)]. The residuals are computed as $\log_{10}(\langle \Delta r^2(t) \rangle / \mathrm{MSD}_{fit})$. Between the black dashed lines in [(b) and (d)], the fits are less than 10% off from the data. Despite having one less parameter, the RBM model fits the low temperature data better than the inherent von Schweidler law. In particular, the RBM fits the simulation data better at long times.

1. von Schweidler fit

MSD simulation data are conveniently fitted to the von Schweidler empirical expression, which emerges from MCT theory,[3,10]

$$\Delta_{vS}(t) = r_0^2 + a(6Dt)^b + 6Dt, \tag{4}$$

in which b is a non-universal exponent. Since our focus is on the inherent dynamics that removes the influence of vibrations leading to the MSD plateau, we define an "inherent" von Schweidler (IvS) law by setting $r_0^2 = 0$ in Eq. (4),

$$\Delta_{IvS}(t) = a(6Dt)^b + 6Dt. \tag{5}$$

Equation (5) can be expressed as $l_0^2\left[(t/\tau_0)^b + t/\tau_0\right]$ in which $l_0^2 \equiv a^{1/(1-b)}$ and $\tau_0 \equiv l_0^2/(6D)$. Thus, Eq. (5) has one dimensionless shape parameter, b. Note that while the IvS is inspired by MCT, the results reported below should *not* be interpreted as a test of MCT: except for $T = 0.652$, all temperatures are below the estimated[13] $T_{\rm mct} \cong 0.62$; the IvS should, thus, in this work merely be considered as a convenient fitting function.

We show in Fig. 3(a) the all-particle inherent MSD curves and their fits to Eq. (5) (data for the A, B, and C particles separately are reported in the Appendix). We ignore the short-time ballistic regime by focusing on times $t > 10$ (LJ units), corresponding to the MSD plateau and diffusive regimes.

At all temperatures and times, the fit appears to be quite good. We quantify the quality of the fit by computing the residuals defined as the (base 10) logarithm of the ratio of the IS MSD to the von Schweidler fit; see Fig. 3(b). When the residuals are positive (resp. negative), the von Schweidler fit underestimates (resp. overestimates) the IS MSD. Within the region delimited by the two dashed lines, the fit is less than 10% off from the data. The quality of the fit deteriorates notably with decreasing temperature and long times.

2. Random barrier model fit

We next turn to the fit to the Random Barrier Model (RBM) prediction. The RBM is a model for the motion of particles in a random environment, characterized by the following simplifying assumptions:[5,6,17]

1. Particles jump stochastically on a cubic lattice in d dimensions.
2. Only nearest-neighbor jumps are possible.
3. All site energies are identical.
4. The particles do not interact, i.e., even self-exclusion at each lattice site is ignored.
5. The link jump rates are proportional to $\exp(-\beta E)$ in which $\beta = 1/k_B T$ and E is an activation energy chosen randomly from a probability distribution, $p(E)$.

The RBM is characterized by a universal time-dependent MSD in the extreme disorder limit defined by $\beta \to \infty$, i.e., when jump rates cover several decades. This means that $\langle \Delta r^2(t) \rangle$ in dimensionless units becomes independent of $p(E)$ in the extreme disorder limit. This universality, which has been validated by extensive simulations,[5,7] follows from the fact that percolation controls the physics in this limit.[7] The only assumption needed is that $p(E)$ is continuous at the energy of the (link) percolation threshold.[5,18]

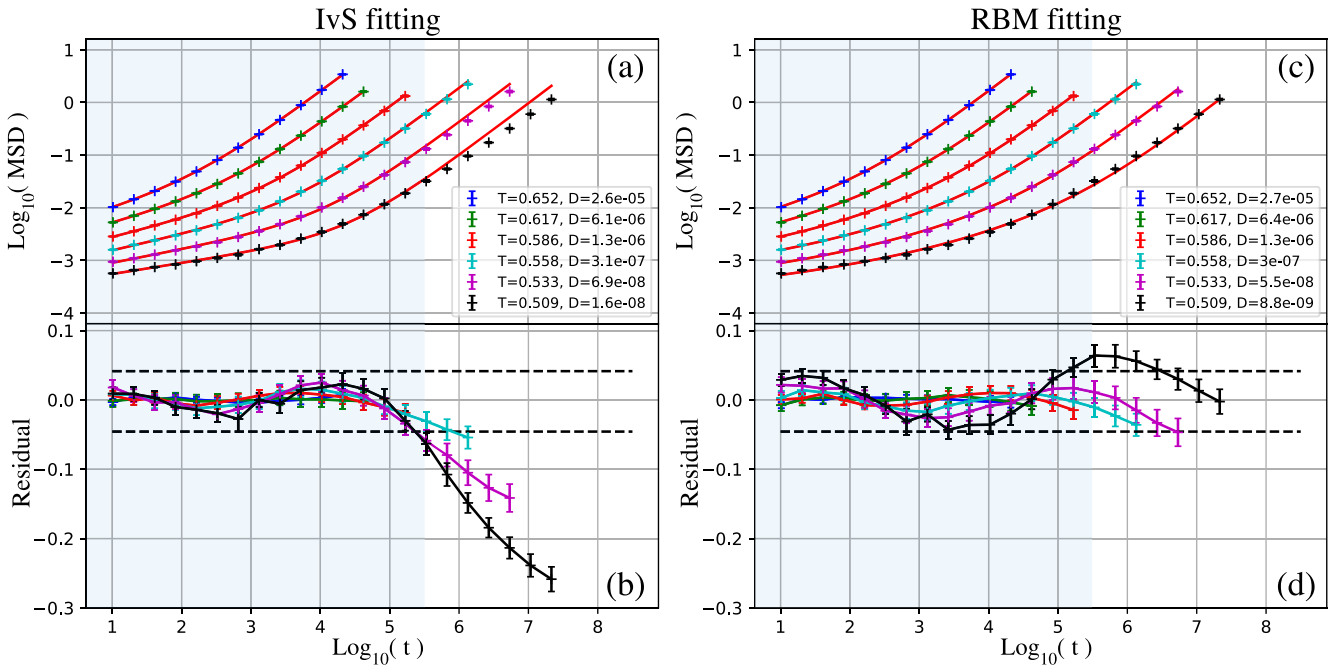

FIG. 4. Same as Fig. 3, except that fits are here restricted to $t < 3 \times 10^5$, highlighted by the shaded region.

The frequency-dependent diffusion coefficient is defined by

$$D(\omega) \equiv (-\omega^2/6)\int_0^\infty \langle \Delta r^2(t)\rangle \exp(i\omega t)dt, \tag{6}$$

see Refs. 19–21. If one defines $\tilde{\omega}$ as a properly scaled frequency and $\tilde{D} \equiv D(\omega)/D(0)$,[7] an accurate analytical approximation to the RBM universal $D(\omega)$ is the solution of

$$\ln \tilde{D} = \left(\frac{i\tilde{\omega}}{\tilde{D}}\right)^{2/3}. \tag{7}$$

This is derived by combining the Alexander–Orbach conjecture—that the percolation cluster has harmonic dimension 4/3 for percolation in any number of dimensions[22]—with the effective-medium approximation (EMA) applied to diffusion on the percolation cluster defined by the smallest activation-energy links.[7] Even though both the EMA and the Alexander–Orbach conjecture are known not to be rigorously correct in all dimensions, the quoted equation provides an excellent fit to computer simulations of the RBM in three dimensions involving jump rates covering many decades.[7] Of particular interest in the present context is that the Alexander–Orbach conjecture is independent of the nature and dimension of the space in which the percolation takes place (the conjecture that the harmonic dimension of the percolation cluster is 4/3 applies rigorously above the upper critical dimension of percolation, which is six,[23] but it is accurate also in lower dimensions). A transition to a frequency-independent diffusion coefficient takes place at low frequencies, corresponding to the long-time $\langle \Delta r^2(t)\rangle \propto Dt$ behavior. In this region, the above RBM analytical approximation needs an extra term to be accurate, and the overall behavior is well described by the solution of the following empirical equation:[7]

$$\ln \tilde{D} = \frac{i\tilde{\omega}}{\tilde{D}}\left(1 + \frac{8}{3}\frac{i\tilde{\omega}}{\tilde{D}}\right)^{-1/3}. \tag{8}$$

[The scaled frequencies in Eqs. (7) and (8) are proportional but not identical.] The Appendix quotes a numerical approximation to the RBM mean-square displacement as a function of time [Eq. (6)] that is accurate over ten decades of time.

We report in Fig. 3(c) the IS MSD along with their best fit to the RBM prediction. To assess the validity of the RBM prediction, we report in Fig. 3(d) the residuals defined as above. Despite having no shape parameters—as compared to the one shape parameter of the von Schweidler expression—the RBM describes the data better. While the two analytical approximations work equally well close to $T_{\rm mct} \sim 0.62$, the error at the lowest temperatures is clearly smaller for the RBM prediction.

D. Predictive power of the two fits

Given that long simulations are computationally costly, one might find it useful to do extrapolations of the data at long times and low temperature. We focus on the IS MSD and use long simulation trajectories to investigate how well the two fitting functions predict the IS MSD at long times. We do this by restricting the fits to shorter times and then comparing the long-time data predicted from the fit to the measured one. The fits were performed over a window $10 < t < 3 \times 10^5$, i.e., two orders of magnitude shorter than the longest simulation. Data, restricted fits, and their residuals are shown in Fig. 4. We see in Fig. 4(a) that the restricted von Schweidler fit significantly departs from the data at long times. This is confirmed by the residuals (b), which plummet at long times and low temperature. The RBM extrapolation is much more accurate; see Figs. 4(c) and 4(d).

The above extrapolation yields a diffusion coefficient, even when the diffusive regime cannot be accessed brute-force by long simulations. This may be useful to test Stokes–Einstein breakdown in the extremely viscous regime, if combined with, e.g., a parabolic law to extrapolate the relaxation time data. We investigate stability and convergence of the estimated diffusion coefficient by restricting the fits over time windows of increasing length. The estimated diffusion coefficient is reported in Fig. 5 for the three lowest temperatures as a function of the longest time included in the fit (the shortest one still being 10 LJ time unit) for both the von Schweidler (curves above the dashed lines) and RBM fits (curves mostly below the dashed lines). Fitting the data over too short time scales yields bad estimates in both cases, and the estimate obviously improves with increasing the fitting time windows. The convergence is much

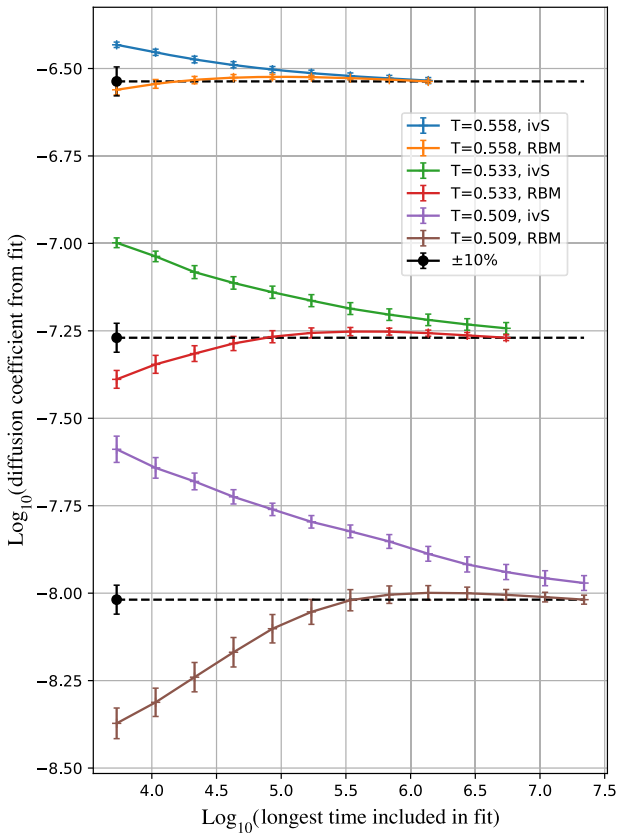

FIG. 5. Diffusion constant obtained by fitting the von Schweidler and RBM predictions to the IS MSD over a time window starting at 10 LJ time units and terminating at the time indicated on the horizontal axis. The horizontal dashed lines highlight the value obtained for fitting the whole trajectory, with the bullet/error bar (left) indicating an error of 10% around it. Temperature decreases from top to bottom.

faster for the RBM fit compared to that of the IvS, however, especially at low temperature where long simulation times are not enough to ensure convergence of the IvS estimate. In comparison, the RBM prediction yields a diffusion coefficient, which varies less than 10% when the fitting window increases by two decades. The fact that the parameter fit, the diffusion coefficient for the RBM prediction, is not very sensitive to the fitting range confirms that it represents well the data over a broad range of temperatures and time scales.

We next study the evolution of the IvS shape parameter, b, with the fitting range. The results are shown in Fig. 6 at our three lowest temperatures, decreasing from top to bottom. The fitting starts at 10 LJ time units and terminates at the value indicated on the horizontal axis. The shape parameter depends significantly on the fitting window. At the lowest temperature, the shape parameter increases by more than 30% when increasing the fitting window by three orders of magnitude, and the shape parameter does not converge over a simulation window of nine decades (the maximum accessible). We interpret this as reflecting that there is no short time power-law as contained in the IvS, since this should eventually lead to an (approximately) constant shape parameter b.

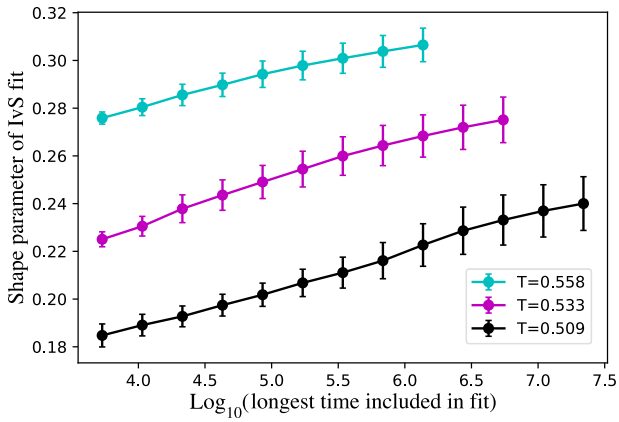

FIG. 6. The shape parameter, b, of the von Schweidler fit to the IS MSD as a function of the maximum time included in the fit. There are few signs of stabilization at long maximum times.

IV. DISCUSSION

The RBM prediction accurately captures the time evolution of the IS MSD down to unprecedentedly low temperatures, extending the findings of Ref. 3 to a regime that is 1.5 decades closer to the experimental glass transition. Moreover, the RBM outperforms the von Schweidler law in its ability to extrapolate the data to longer times and reliably extract the diffusion coefficient. This is notable in view of the fact that the RBM has no shape parameters, in contrast to the von Schweidler law that has one shape parameter.

What do our results tell about the possible universality discussed in Sec. I? We have shown that the IS MSD is well reproduced by the RBM prediction. Once the IS MSD data are rescaled by a parameter c with dimension of a length squared and time by $c/(6D)$, the curves collapse for all temperatures investigated, see Fig. 7 (plus symbols). The corresponding plots for A, B, and C particles separately are given in the Appendix. This implies that time–temperature superposition applies to the IS MSD and, importantly, that the IS MSD of the studied model adheres to the possible universality discussed in Sec. I.

Figure 7 also shows the true/thermal MSD data (dashed lines), scaled using the parameters obtained from the IS MSD. In contrast to the binary model studied in Ref. 3, the true/thermal MSD does *not* collapse onto a master curve under this scaling procedure. This suggests that the additive constant β introduced in Ref. 3 to account for intermediate-time cage rattling is not universal and likely exhibits a significant temperature dependence. Such non-universality may explain why the apparent RBM universality was not identified previously, since most studies focused on the thermal MSD rather than the IS MSD.

Finally, we present selected data on a third, polydisperse LJ model, whose structural relaxation dynamics has been analyzed

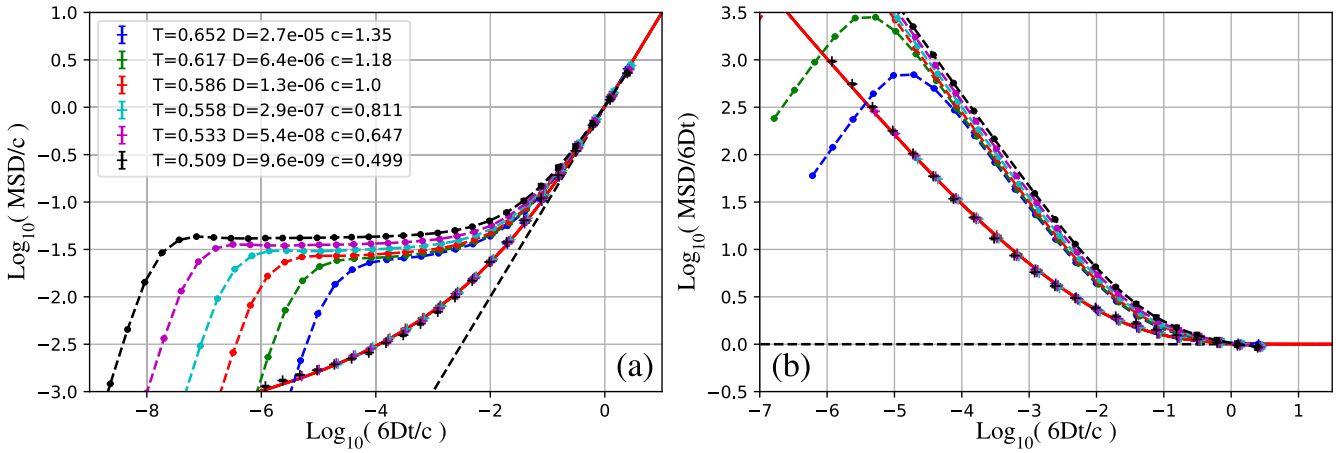

FIG. 7. (a) True and inherent all-particle MSD scaled by D and c as estimated by RBM fits. Red full curve: RBM prediction of the inherent MSD. (b) Same data divided by $6Dt$.

down to the extrapolated experimental glass transition.[16] We performed the RBM analysis for the IS MSD of this additional model. Figure 8 shows the thermal and IS data (a), and rescaled by D and c (b). While the present IS MSD data for the polydisperse model is more noisy, we again find an overall good agreement with the RBM for all temperatures studied. This significantly increases the regime of validity of the RBM scaling, since the lowest temperature studied $T = 0.059$ has an extrapolated relaxation time, which is 11 decades larger than at the onset temperature of glassy dynamics, i.e., almost at the experimental glass transition temperature typically defined by a 12-decade slowdown (almost seven decades slower than MCT). The polydisperse model also has the property that the intermediate-time additive constant is non-universal; see Fig. 8(b).

In Fig. 8(c), the RBM estimate of the diffusion coefficient is about 0.1 decade (corresponding to roughly 25%) too big when compared to the long-time limit of the simulation data. In comparison, the diffusion coefficient changes by more than a factor of 1000 over the temperature interval studied. Looking closely at Fig. 7(b), we see that extrapolating the data by eye suggests a similar behavior for the ternary model. Exactly where the small deviations are found depends on how the RBM fit is performed. For the data in Figs. 7 and 8, the RBM fit was used to estimate the two scaling parameters D and c simultaneously. In contrast, for the binary system in Ref. 3 where all state points had a well-defined diffusive regime, the diffusion coefficient was first estimated by fitting the long time MSD, and only after this was c estimated by fitting to the RBM prediction. Unsurprisingly, this procedure gives estimates of the diffusion coefficient consistent with the long-time limit of the simulation data. We cannot apply this procedure to the polydisperse system, since the diffusional regime can only be reached for a few of the state points. What we can do instead is to put a constraint on the fitted diffusion coefficient so that the MSD for the last data point for each temperature is *not* smaller than $6Dt$. The result of this procedure is shown in Fig. 9, now showing good consistency between the diffusion coefficients and the long-time limit of the simulation data.

In summary, three different model liquids show very good—though not perfect—agreement between the inherent MSD

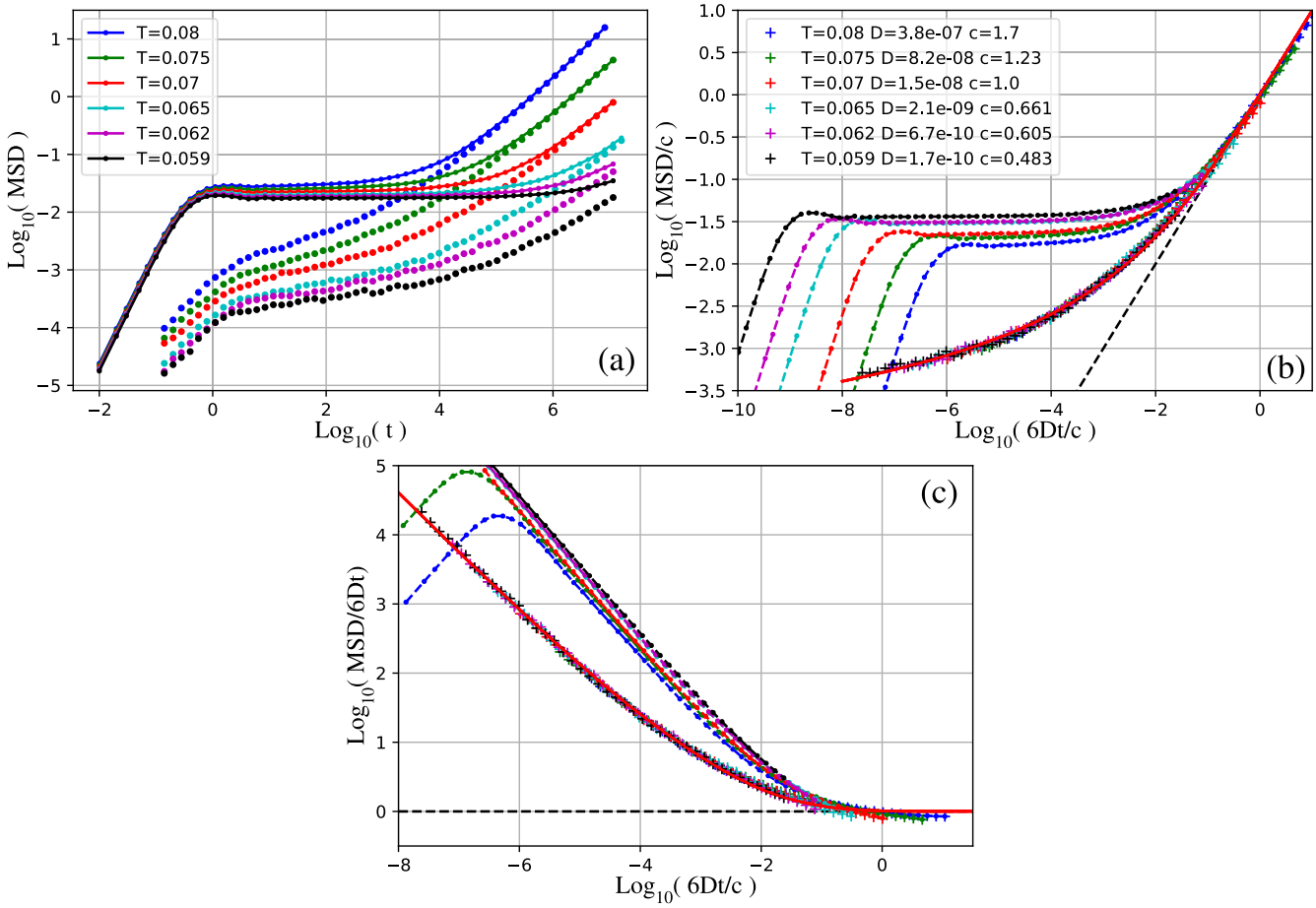

FIG. 8. (a) True and inherent all-particle MSD for a polydisperse LJ model.[16] (b) Same data, scaled by D and c as estimated by RBM fits. Inherent data only used for $t > 10$. Red full curve: RBM prediction of the inherent MSD. (c) Same as (b) but with the y axis divided by $6Dt$.

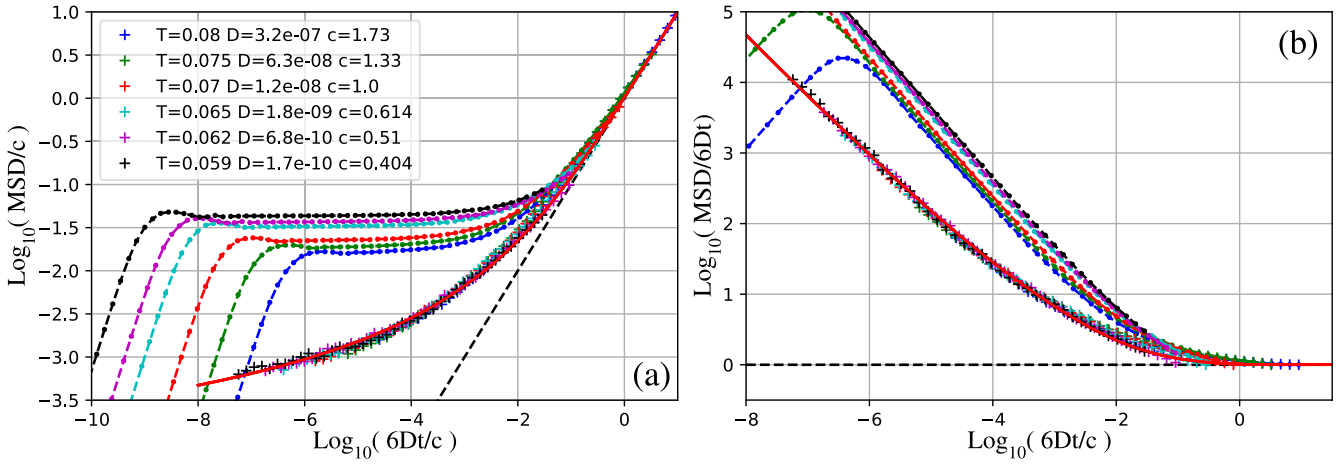

FIG. 9. Same data as in Fig. 8, but with the RBM fit performed with the constraint on the diffusion coefficient that the MSD for the last point for each temperature is *not* allowed to be smaller than 6*Dt*.

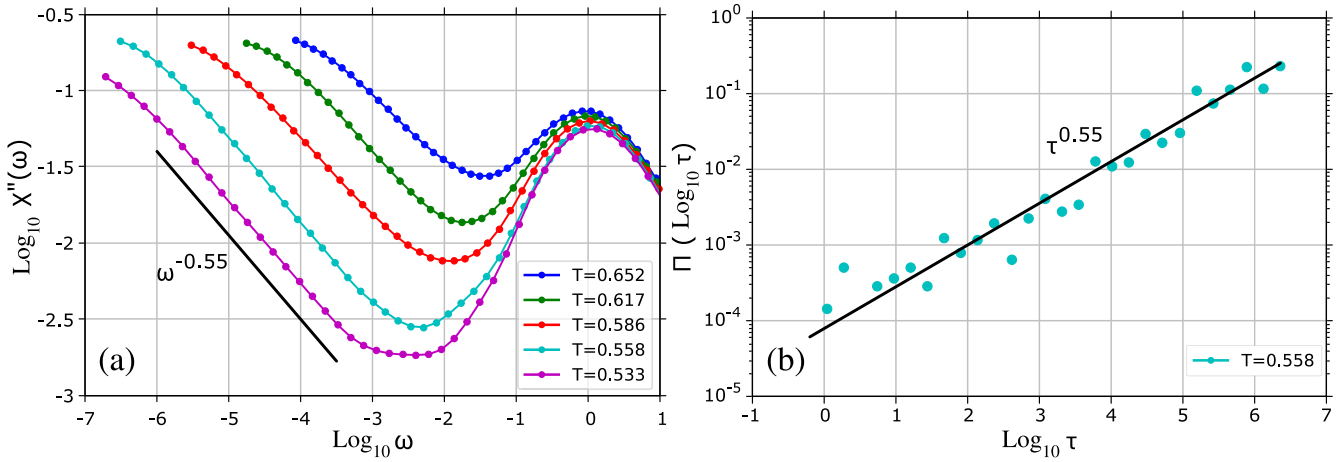

FIG. 10. Relaxation spectra and apparition of mobile regions in the ternary model. (a) Relaxation spectra $\chi''(\omega)$ as a function of frequency ω, defined from the self-intermediate scattering function. The data reveal an "excess wing," as observed in the polydisperse model, yet with a different exponent, here 0.55 (0.47 for temperatures of comparable diffusion coefficient in the polydisperse model). (b) Probability distribution Π of the time τ at which new mobile regions appear in the liquid. The distribution is characterized by the same exponent 0.55.

and the RBM prediction. This is remarkable in view of the fact that the RBM has no shape parameters in the extreme disorder limit. It might be tempting to think that these models are very similar; after all, they are atomic Lennard-Jones liquids with two, three, and many types of particles. Figure 10 shows, however, that in regard to relaxation, the ternary model is quantitatively different from the polydisperse model. We reproduce here the analysis performed in Ref. 16 on the polydisperse model for the ternary one: we compute the relaxation spectra $\chi''(\omega)$ defined from the self-intermediate scattering function. We find that the relaxation spectra of the ternary model also exhibit power-law scaling at high frequency, $\chi''(\omega) \sim \omega^{-\sigma}$. The exponent found at low temperature, $\sigma \simeq 0.55$, is, however, different from that found in the polydisperse model. For temperatures where the diffusion coefficient is the same as those shown in Fig. 10, $D \sim 10^{-7}$, the spectra, indeed, follow a different exponent in the polydisperse model, $\sigma \simeq 0.47$. Still, we confirm that the power-law in the spectra arises from the apparition of mobile regions, which occurs over very broadly distributed time scales. Indeed, Fig. 10(b) shows that the probability distribution of the time τ at which new mobile regions appear exhibits a power-law with the same exponent. We conclude that the relaxation process is qualitatively similar, yet quantitatively different, in the two

models: mobility starts in rare regions over broad time scales, which are known to then slowly grow in time. This observation is interesting because the short-time signal in the IS MSD—well described by the RBM in the two models—is directly caused by the apparition of these rare mobile regions, yet characterized by different exponents.

More work is needed to determine whether the RBM is a truly universal representation of the inherent MSD of highly viscous glass-forming liquids. In particular, it would be interesting to investigate molecular models, which has recently become possible by swap methods.[24,25] If the RBM applies universally, an important theoretical challenge arises of explaining why it works so well. The point is that hopping of non-interacting particles in a random landscape, i.e., with both varying minima and maxima does not conform to the RBM universality prediction, which requires identical minima. The latter would lead to a zero "inherent" specific heat (the contribution to the specific heat from jumping between different potential-energy minima) and no decrease in the specific heat when the liquid is cooled through the glass transition. This contradicts numerous experiments. This also leads to the question of whether the RBM is to be thought of as reflecting some sort of mean-field behavior in three dimensions or in the high-dimensional configuration space. The former possibility was very recently discussed by Maass and co-workers, who studied numerically the effect of self-exclusion (Fermi statistics) for a system of particles hopping in a landscape on a lattice with random site energies.[26] Their work demonstrates that the RBM gives an excellent representation of the time-dependent mean-square displacement; apparently, Fermi statistics restores RBM universality. The situation is far from clear and understanding why the RBM works to well is an important theoretical challenge for future works.

ACKNOWLEDGMENTS

This work was supported by the VILLUM Foundation's *Matter* Grant (No. VIL16515). The authors thank Ludovic Berthier for helpful suggestions and discussions and Benjamin Guiselin for providing IS MSD data of the three-dimensional polydisperse model.

AUTHOR DECLARATIONS

Conflict of Interest

The authors have no conflicts to disclose.

Author Contributions

Thomas B. Schrøder: Conceptualization (equal); Methodology (equal); Writing – original draft (equal); Writing – review & editing (equal). **Jeppe C. Dyre**: Conceptualization (equal); Writing – original draft (equal); Writing – review & editing (equal). **Camille Scalliet**: Methodology (equal); Writing – original draft (equal); Writing – review & editing (equal).

DATA AVAILABILITY

The data that support the findings of this study are available from the corresponding author upon reasonable request.

APPENDIX: ANALYSIS RESTRICTED TO PARTICLE TYPES, AND RBM SOLUTION IN THE TIME DOMAIN

Figure 11 reports data identical to Fig. 7, except that the averages are restricted to A, B, C particles, respectively.

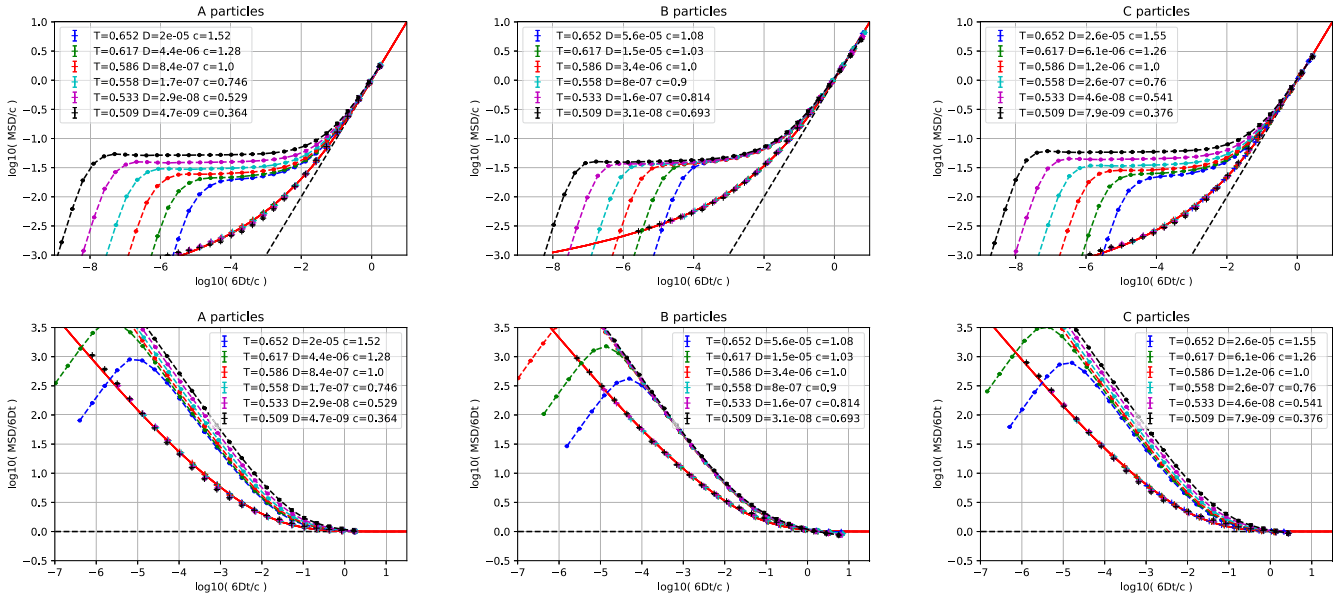

FIG. 11. Upper panels: True and inherent MSDs scaled by D and c as estimated by RBM fits for A, B, and C particles, respectively. Red full curve: RBM prediction of the inherent MSD. Lower panels: Same data divided by 6*Dt*.

The Random Barrier Model (RBM) was solved numerically in the real-Laplace-frequency domain on a cubic lattice with a box distribution of energy barriers.[7] At low temperatures, the shape of the frequency-dependent diffusion coefficient $D(s)$ for the RBM becomes universal, i.e., independent of temperature and energy barrier distribution.[18] $D(s)$ for $\beta = 320$ where β is the maximum barrier over the temperature was found to be a good representation of the universal RBM prediction that is accurately represented by Eq. (8).

To facilitate transformation from the real-Laplace-frequency domain to the time domain over the many decades involved, we fit to the following empirical fitting function in which $\tilde{s} \equiv s/D(0)$,

$$\frac{D(\tilde{s})}{D_0} = 1 + \sum_{j=1}^{10} a_j \tilde{s}^{j/10}. \tag{A1}$$

The fitting was performed after taking the logarithm of both the numerical data and the fitting function, resulting in the following parameters $(a_1, \ldots, a_{10}) = (-1.1914,\ 11.2368,\ -34.2903,\ 26.6019,\ 47.0002,\ -96.2905,\ 77.4671,\ -27.0535,\ 7.725\,35,\ -0.178\,844)$.[3]

Using $D(s) \equiv (s^2/6)\int_0^\infty \langle \Delta r^2(t)\rangle \exp(-st)dt$ (see the main text), Eq. (A1) implies

$$\langle \Delta r^2(\tilde{t})\rangle = 6D_0\tilde{t}\left(1 + \sum_{j=1}^{10} \frac{a_j \tilde{t}^{-j/10}}{\Gamma(2 - j/10)}\right). \tag{A2}$$

This is the equation used to represent the RBM mean square displacement. Equation (A2) corrects a typo in Eq. (A2) of Ref. 3 in which the term $\tilde{t}^{-j/10}$ erroneously appeared as $\tilde{t}^{1-j/10}$ (this was corrected in an Erratum at the time).

REFERENCES

[1] S. P. Bierwirth, R. Böhmer, and C. Gainaru, "Generic primary mechanical response of viscous liquids," Phys. Rev. Lett. **119**, 248001 (2017).

[2] C. Gainaru, "Spectral shape simplicity of viscous materials," Phys. Rev. E **100**, 020601 (2019).

[3] T. B. Schrøder and J. C. Dyre, "Solid-like mean-square displacement in glass-forming liquids," J. Chem. Phys. **152**, 141101 (2020).

[4] T. B. Schrøder, S. Sastry, J. C. Dyre, and S. C. Glotzer, "Crossover to potential energy landscape dominated dynamics in a model glass-forming liquid," J. Chem. Phys. **112**, 9834–9840 (2000).

[5] T. B. Schrøder and J. C. Dyre, "Universality of ac conduction in disordered solids," Rev. Mod. Phys. **72**, 873–892 (2000).

[6] J. C. Dyre, "The random free-energy barrier model for ac conduction in disordered solids," J. Appl. Phys. **64**, 2456–2468 (1988).

[7] T. B. Schrøder and J. C. Dyre, "Ac hopping conduction at extreme disorder takes place on the percolating cluster," Phys. Rev. Lett. **101**, 025901 (2008).

[8] A. D. S. Parmar, M. Ozawa, and L. Berthier, "Ultrastable metallic glasses in silico," Phys. Rev. Lett. **125**, 085505 (2020).

[9] N. Bailey, T. Ingebrigtsen, J. S. Hansen, A. Veldhorst, L. Bøhling, C. Lemarchand, A. Olsen, A. Bacher, L. Costigliola, U. Pedersen, H. Larsen, J. Dyre, and T. Schrøder, "RUMD: A general purpose molecular dynamics package optimized to utilize GPU hardware down to a few thousand particles," Scipost Phys. **3**, 038 (2017).

[10] W. Kob and H. C. Andersen, "Testing mode-coupling theory for a supercooled binary Lennard-Jones mixture I: The van Hove correlation function," Phys. Rev. E **51**, 4626–4641 (1995).

[11] S. Sastry, "Liquid limits: Glass transition and liquid-gas spinodal boundaries of metastable liquids," Phys. Rev. Lett. **85**, 590–593 (2000).

[12] V. Testard, L. Berthier, and W. Kob, "Influence of the glass transition on the liquid-gas spinodal decomposition," Phys. Rev. Lett. **106**, 125702 (2011).

[13] F. C. Mocanu, L. Berthier, S. Ciarella, D. Khomenko, D. R. Reichman, C. Scalliet, and F. Zamponi, "Microscopic observation of two-level systems in a metallic glass model," J. Chem. Phys. **158**, 014501 (2023).

[14] L. Berthier, E. Flenner, C. J. Fullerton, C. Scalliet, and M. Singh, "Efficient swap algorithms for molecular dynamics simulations of equilibrium supercooled liquids," J. Stat. Mech.: Theory Exp. **2019**, 064004.

[15] F. H. Stillinger and T. A. Weber, "Dynamics of structural transitions in liquids," Phys. Rev. A **28**, 2408–2416 (1983).

[16] C. Scalliet, B. Guiselin, and L. Berthier, "Thirty milliseconds in the life of a supercooled liquid," Phys. Rev. X **12**, 041028 (2022).

[17] J. C. Dyre, "A simple model of ac hopping conductivity in disordered solids," Phys. Lett. A **108**, 457–461 (1985).

[18] T. B. Schrøder and J. C. Dyre, "Scaling and universality of ac conduction in disordered solids," Phys. Rev. Lett. **84**, 310–313 (2000).

[19] J. W. Haus and K. W. Kehr, "Diffusion in regular and disordered lattices," Phys. Rep. **150**, 263–406 (1987).

[20] J.-P. Bouchaud and A. Georges, "Anomalous diffusion in disordered media: Statistical mechanisms, models and physical applications," Phys. Rep. **195**, 127–293 (1990).

[21] J. C. Dyre and T. B. Schrøder, "Hopping models and ac universality," Phys. Status Solidi B **230**, 5–13 (2002).

[22] S. Alexander and R. Orbach, "Density of states on fractals: 'fractons,'" J. Phys. Lett. **43**, 625–631 (1982).

[23] B. D. Hughes, *Random Walks and Random Environments* (Clarendon, Oxford, 1996).

[24] T. Böhmer, J. C. Dyre, and L. Costigliola, "Swap Monte Carlo for diatomic molecules," Phys. Rev. E **112**, 035402 (2025).

[25] R. Simon, J.-L. Barrat, and L. Berthier, "Molecular motion at the experimental glass transition," Phys. Rev. X **16**, 011035 (2026).

[26] S. Lohmann, Q. E. Fischer, J. Leiber, and P. Maass, "Universal time-temperature scaling of conductivities in random site energy and associated random barrier models," Phys. Rev. B **113**, 184201 (2026).